SDSS'Rio 2010 STABILITY AND DUCTILITY OF STEEL STRUCTURES
E. Batista, P. Vellasco, L. de Lima (Eds.)
Rio de Janeiro, Brazil, September 8 - 10, 2010

THE COLLAPSE LOAD IN SUBMARINE PIPELINES UNDER COMPRESSIVE LOAD AND INTERNAL PRESSURE

LUCIANO M. BEZERRA*, RAMON S. Y. C. SILVA*

* Department of Civil Engineering, University of Brasilia, 70910-900 – Brasilia, DF - Brazil
e-mails: lmbz@unb.br, ramon@unb.br

Keywords: Pipeline Collapse Load, Pressurized Pipelines, Petroleum Pipelines.

Abstract. *In off-shore plataform, petroleum from the oil well may have to be heated up so that its density decrease, making easier the pumping of petrolium along pipelines. Due to temperature increase, such pipelines may be under thermal dilatation and, consequently, under high compressive thermal loading. There is a great difficult in finding the collapse load of such submarine pipeline. An analytical method is presented in this paper for the determination of the collapse load of pressurized pipelines extended over large free spans. The collapse load is determined from a closed solution equation. Results of the presented formulation are compared with sophisticated finite element analyses. For the determination of the collapse load of pressurized freespan pipelines under compression, non-linear finite element analysis requires a lot of computer processing while the present formulation takes practically no time to assess a good approximation for the collapse load.*

NOTATION

A_o = Area of pipe cross-section
A_c = Section area under compressive stress
A_t = Section area under tensile stress
BP = Buried pipeline
E = Modulus of Elasticity
FSP = Freespan pipeline
Fc = Compressive cross-sectional force
F_t =Tensile cross-sectional force
I = Moment of Inertia of cross-section
L = Length of freespan
M(x) = Bending moment in the pipe
M_p = Fully plastic bending moment
M^{θ}_{pc} = Fully plastic moment capacity in the presence of P and σ_θ
P = Axial load at freespan ends
p = Internal/external pressure in pipe
P_E = Euler critical load
P_{cr} = Critical axial load for collapse
P_s = Force in centerline spring support
$\bar{P}$ = FSP collapse load
R or r = External or Internal radius of pipe
$\bar{y}_c\,(\bar{y}_t)$ = Centroid of A_c (A_t) w.r.t. x-x (Fig. 5)
(x,y,z) = 3D right-handed coordinate system
(u,v,w) = Displacements associated w/(x,y,z)
Z = Plastic section modulus
w = Beam's transverse displacement
α = Arm inclination/for model without initial imperfection (Fig. 2)
β = Arm inclination/for model with initial imperfection (Fig. 3)
δ = Arm lateral deflection at centerline
σ = Compressive longitudinal stress=P/A_o
σ_E = Euler critical stress = P_E / A_o
σ_c = Compressive longitudinal stress on A_c
σ_t = Tensile longitudinal stress on A_t
σ_y = Yielding stress
σ_u = Ultimate stress
$\bar{\sigma}$ = FSP collapse stress = P_{cr} / A_o
σ_1 = Von-Mises longitudinal stress
σ_θ = Von-Mises circumferential stress
ρ = Radius of curvature of pipe bending
ψ = Angle enveloping the area A_t (Fig. 5)
ϕ = Angular cross-sectional coordinate
$\xi\,(\eta)$ = Non-dimensional hoop (longitudinal) stress

1. INTRODUCTION

Submarine pipelines are often laid on relatively rough sea-bottom terrains and, consequently, may be supported by soil only intermittently, without intermediate support. Such spans are identified as "freespans". The scope of this paper is to predict the behavior of freespan pipelines under compressive loads originating from effects such as temperature differentials. The paper deals exclusively with free span pipelines under compressive load combined with internal pressure. The compressive load, P, is assumed to be applied at the ends of the pipe segment and to be collinear with a line through the end supports of the pipe segment. Consequently, the load is considered to act along the chord connecting the two ends of the freespan segment, without change in the load direction. The collapse mechanics of a segment of a free span pipeline (FSP) under compressive load is not necessarily the same as for a buried pipeline (BP). Adequate support around a BP may prevent it from buckling globally. Assuming a FSP under compression deforms as shown in Fig.-1, the collapse mode of a FSP under compression, depends upon the length of the free span, and will be different than for local wrinkle formation typically observed in short segments of BPs. For short free span lengths, the collapse mode of the FSP might be similar to the local wrinkle formation mode observed in BPs. For long free spans, the collapse mode might be comparable to the global buckling collapse mode observed in a structural column.

2. THE PIPE AND THE MODEL

Assuming small deformation theory, a long FSP, if ideally straight, elastic, and isotropic, loaded along the central axis, should behave like any long structural member under compression. The first model that comes to our mind is the buckling of the Euler's column. For all practical purposes, the prescribed Euler's collapse load in Eq.(1) for a pinned-end column is an upper limit of compressive loading for an ideal FSP.

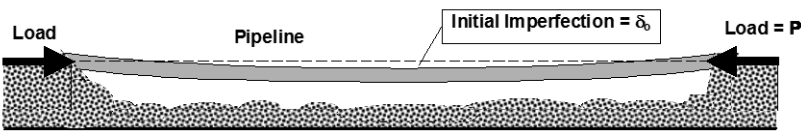

Figure-1: Freespan pipeline under compressive load and initial imperfection δ_0.

$$P_E = \frac{\pi^2 EI}{L^2} \tag{1}$$

To determine a more realistic behavior of FSPs under compressive load it is necessary to admit the existence of initial imperfections, the possibility of inelastic behavior, and the mobilization of fully plastic moment capacity of the pipe section. Let us consider the effect of initial imperfection and plastic deformations, using the mechanical model shown in Fig.-2 [6]. Subsequently, it is possible to examine for the effects of initial imperfection and inelastic material behavior on the buckling behavior. The mathematical model consists of two rigid arms pinned together at the span center-line at C. On the ends (A and B) they are pinned too, as in Fig.-3. A vertical spring, with stiffness K, is attached at C. Applying an increasing horizontal axial force P at point A through the centroidal cross-sectional axis, with $\delta = 0$, will make P reaches its critical load, P_{cr}.

At this critical load, when buckling takes oplace, the model forms a mechanism in which point C displaces laterally through a distance δ, and the arm rotates α - see Fig.-2b. Prior to instability, the force in the spring, $P_s = 0$. As soon as the instability takes place, $P_s = K\delta$ - with K being the spring constant. From moment equilibrium of the arm from A to C, about C, for Fig.-2b, we can write for small angles

$$P_{cr}\delta = \left(\frac{P_S}{2}\right)\left(\frac{L}{2}\right) \quad \text{or} \quad \frac{P_{cr}}{P_s} = \frac{L}{4\delta} \tag{2}$$

In Fig.-2a, to simulate the Euler's buckling load, the lateral defection δ will take place abruptly when the critical load reaches the Euler's load. Substituting $K\delta$ for P_s in Eq. (2) and equating $P_{cr} = P_E$ yelds

$$P_{cr} = P_E = \frac{KL}{4} \quad \text{or} \quad K = \frac{4P_E}{L} \tag{3}$$

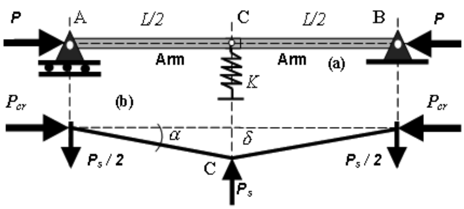

Figure-2: (a) An elementary buckling model and (b) free-body diagram.

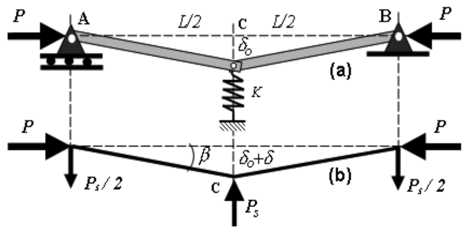

Figure-3: The mechanical model with initial imperfection.

Up to now, the pre-buckling shape is a straight line, however, by now let's consider the existence of an initial imperfection $\delta o \neq 0$ in Fig.-3. Note that small initial imperfections will be amplified by the axial force. The model of the FSP with an initial imperfection δo is in Fig.-3a. δo exists initially, for P = 0 and $P_s = 0$. For $P \neq 0$, the incremental displacement at the centerline increases by the amount δ due to the rotation of the arms – see Fig.-3a. The total displacement, due to the arm rotation, β, becomes $\delta_{tot} = \delta_0 + \delta$ - Fig.-3b. The moment equilibrium of arm A-C, about C, for Fig.-3b may be expressed by Eq.(4).

$$P\delta_{tot} = \left(\frac{P_S}{2}\right)\left(\frac{L}{2}\right) \quad \text{or} \quad \delta_{tot} = \left(\frac{P_s L}{4P}\right) \quad \text{and} \quad \delta_{tot} = \delta_o + \delta \tag{4}$$

A_s $P_S = K\delta$ and $\delta = \delta_{tot} - \delta_0$, and using Eq.(3) for K; Eq.(4) can be transformed into the following equation

$$\delta_{tot} = \left(\frac{P_s L}{4P}\right) = \left(\frac{KL\delta}{4P}\right) = \left(\frac{4P_E L\delta}{4P}\right) = \left(\frac{P_E}{P}\right)\left(\delta_{tot} - \delta_o\right) \quad \text{or} \quad P = \left(\frac{1-\delta_0}{\delta_{tot}}\right)P_E \tag{5}$$

The model for the FSP with an initial δo will result in an increase in bending moment at the center of the span as P and δ_{tot} increase. However, P in Eq. (5) indicates that the compressive load for the model of the imperfect column (or FSP) will never reach the Euler's load, P_E, but approaches P_E asymptotically. In addition, the maximum bending moment that can arise at the central section cannot exceed that associated with the fully plastic condition for the pipe. At the central section $M = P\delta_{tot}$ and the collapse load for can be determined by the load P that produces the moment which, when combined with the axial effects, mobilizes the fully plastic capacity of the pipe section (M^{θ}_{pc}). To compute the full plastic capacity of the pipe it is necessary a yield criterion.

Pressurized pipes are subjected to hoop and longitudinal stresses due to axial forces and transverse bending moments acting on the pipe cross section. For a thin-walled pipe, the hoop stress is considered constant and stresses other than hoop and longitudinal may be neglected. The longitudinal stress σ_l and the hoop stress σ_θ are identified as the principal stresses σ_1 and σ_2, respectively. Using the Von-Mises-

Hencky yield criterion (with σ_y as the uniaxial yield strength) the maximum (and minimum) longitudinal stresses that the fully-plastic pipe cross section can sustain on the cross section may be calculated as

$$\left(\frac{\sigma_l}{\sigma_y}\right)=\left(\frac{2\sigma_\theta}{\sigma_y}\right)\pm\sqrt{1-\left(\frac{3}{4}\right)\left(\frac{\sigma_\theta}{\sigma_y}\right)^2} \tag{6}$$

Eq.(6) is also valid for the ultimate stress (σ_u) in the place of the yielding stress (σ_y). Eq.(6) also identifies the two values of σ_l that produce yielding for a specified σ_θ. One corresponds to a compressive stress ($\sigma_l = \sigma_c$), and the other, to a tensile stress ($\sigma_l = \sigma_t$) - Fig 4. These values represent the maximum longitudinal compressive and maximum longitudinal tensile stresses that can be developed on the extreme fibers of the pipe cross-section for the given σ_θ. If $\sigma_\theta = 0$, then, for yielding, $\sigma_l=\sigma_c=\sigma_t=\sigma_y$. If $\sigma_\theta \neq 0$, then, the longitudinal stress σ_l required to origin yield in tension is $\sigma_l = \sigma_t$ which is different than that required in compression ($\sigma_l = \sigma_c$) (See Fig.4). Naming $\xi = \sigma_\theta / \sigma_l$ and $\eta = \sigma_l / \sigma_y$, the Von-Mises-Hencky yield criterion is shown in Fig.-4 [4, 5]. From Fig.-4 and Eq.(6), the extreme values for σ_l and σ_θ. For the determination of the fully-plastic capacity of the pipe section, we will assume that the stress-strain curve shows a well defined yield-stress plateau. The yield stress is an important engineering property in order to establish limits on the longitudinal and hoop stresses. The hoop stress σ_θ is given by

$$\sigma_\theta=\frac{pr}{(R-r)} \tag{7}$$

The longitudinal stress acting on the pipe cross-section will depend on the axial force P and the bending moment. The limiting combinations of axial force and bending moment that develop the fully plastic capacity of the pipe section can be presented on an interaction diagram due to [2, 3]. In the following Section, the equations for the fully plastic moment capacity of the FSP pipe section will be derived.

3. DEVELOPING THE FULLY PLASTIC MOMENT

For a pipe, Fig.-5 shows the fully plastic stress distribution, accounting for the effects of stresses σ_t and σ_c [2]. As the pipe is under compressive load P applied at the pipe ends, the applied force is concentrically distributed on the pipe end sections with area A_o giving rise to an equivalent longitudinal uniform stress $\sigma = P/A_0$ at points A and B of Fig.-3, therefore

$$\sigma=\frac{P}{A_0}=\frac{P}{\left[\pi\left(R^2-r^2\right)\right]} \tag{8}$$

The stresses on the pipe section at the point of maximum moment are in Fig.-5 which is a fully plastic condition. At such a point, at the center of the span, we have a combination of stress from bending moment plus stress from axial loading. However, at the ends of the FSP (see Fig.-1 and 3); the force P acts in concert with the transverse force of $P_s/2$, and the combination of these loads must be equilibrated by the stress distribution of Fig.-5 at the centerline of the span. Therefore, at the point of maximum moment, the resultant longitudinal force given by the difference between the tensile force $F_t = \sigma_t A_t$ and compressive force $F_c = \sigma_c A_c$, in Fig.-5, must be in equilibrium with the external applied force P at the ends of the FSP. The areas A_o, A_t, and Ac in Fig.-5 can be expressed as

$$A_o=\pi\left(R^2-r^2\right),\ A_t=\left(\frac{\psi}{2}\right)\left(R^2-r^2\right)\text{ and }A_c=\left(R^2-r^2\right)\left[\left(\frac{(2\pi-\psi)}{2}\right)\right] \tag{9}$$

From Eqs. (8) and (9) we can write the following longitudinal equilibrium equation

$$P = \sigma\pi\left(R^2 - r^2\right) = F_c - F_t = \sigma_c\left(R^2 - r^2\right)\left[\frac{(2\pi - \psi)}{2}\right] - \sigma_t\,(R^2 - r^2)\left(\frac{\psi}{2}\right) \tag{10}$$

The angle ψ can be calculated as a function of the stresses σ, σ_t, and σ_c of Eq.(10).

$$\psi = 2\pi\left[\left(\frac{(\sigma_c - \sigma)}{(\sigma_c + \sigma_t)}\right)\right] \tag{11}$$

A search for P (that causes the stress distribution depicted in Fig.-5) is the same as a search for the equivalent stress $\sigma = P/A_o$ at the end of the FSP. The arms $\bar{y}_t$ & $\bar{y}_c$ of the respective forces F_t and F_c, such forces are at the centroids of the areas A_t and A_c in Fig.-5 - can be calculated as

$$\bar{y}_t = \left[\left(\frac{4\left(R^3 - r^3\right)sin\left(\frac{\psi}{2}\right)}{3\psi\left(R^2 - r^2\right)}\right)\right] \text{ and } \bar{y}_c = \left[\left(\frac{4\left(R^3 - r^3\right)sin\left(\frac{\psi}{2}\right)}{3\left(2\pi - \psi\right)\left(R^2 - r^2\right)}\right)\right] \tag{12}$$

Knowing A_t, A_c in Eq.(9); $\bar{y}_t$, $\bar{y}_c$ in Eq.(12); and σ_c and σ_t in Eq.(6); the maximum plastic resisting moment $M^\theta{}_{pc}$ can be determined due to the load P (or stress σ) at the ends of the FSP. $M^\theta{}_{pc}$ is in equilibrium with the moment caused by the external force P and the eccentricity δ_{tot} of Fig.-3 and Eq.(4), therefore

$$M^\theta{}_{pc} = F_c\bar{y}_c + F_t\bar{y}_t = \sigma_c A_c\bar{y}_c + \sigma_t A_t\bar{y}_t = P\delta_{tot} = \sigma A_o\,\delta_{tot} \tag{13}$$

Using Eqs.(9), and (12) in Eq.(13), the expression for the maximum plastic bending moment is

$$\begin{aligned} M^\theta{}_{pc} = {} & \sigma_c\left(\frac{2\pi - \psi}{2}\right)\left(R^2 - r^2\right)\frac{4\left(R^3 - r^3\right)}{3\left(2\pi - \psi\right)\left(R^2 - r^2\right)}sin\left(\frac{\psi}{2}\right) + \\ & + \sigma_t\left(\frac{\psi}{2}\right)\left(R^2 - r^2\right)\frac{4\left(R^3 - r^3\right)}{3\psi\left(R^2 - r^2\right)}sin\left(\frac{\psi}{2}\right) \end{aligned} \tag{14}$$

Substituting into Eq.(14) the expression for the angle Ψ from Eq.(11), we arrive at the following simplified version of Eq.(14) which is an expression for the maximum moment capacity for the FSP

$$M^\theta{}_{pc} = \left(\frac{2}{3}\right)\left(\sigma_t + \sigma_c\right)\left(R^3 - r^3\right)sin\left[\left(\frac{\pi\left(\sigma_c - \sigma\right)}{\left(\sigma_c + \sigma_t\right)}\right)\right] \tag{15}$$

4. THE PLASTIC COLLAPSE

The limiting fully plastic moment for the FSP as expressed in Eq. (15) is an upper bound on the moment that can be developed before a plastic collapse buckling mechanism occurs. For this mechanism to occur we note that $M^\theta{}_{pc}$ is a function of: (a) the maximum allowable longitudinal stresses, σ_t and σ_c; and (b) the equivalent applied stress σ (or load P, since $\sigma = P/A_0$) applied at the ends of the FSP. It is assumed that a structure with an initial imperfection and under increasing applied compressive load will deform until its fully plastic moment capacity is developed. The expression for maximum moment capacity in Eq.(15) shows that for an increase in σ, there will be a decrease in M^{θ}_{pc} at center span. The formulation contained, herein, is based upon the argument that, to find the compressive collapse stress σ of a FSP, the effect of out-of-straightness must be taken into account. In reality, every structure has imperfections in geometry; but long structures like FSP laid on rough terrains, are more susceptible. The initial imperfection δ_0 is taken into account in Eq.(5). Such equation represents the behavior of the FSP in the elastic range until the fully plastic stress distribution of Fig.-5 is developed giving rise to Eq.(13). Note that Eq.(5), expressed in terms of Euler's critical stress $\sigma_E = P_E/A_0$, can give an expression for δ_{tot} as

$$\sigma = \frac{P}{A_o} = \left[1-\left(\frac{\delta_0}{\delta_{tot}}\right)\right]\left(\frac{P_E}{A_o}\right) \text{ or } \sigma = \left[1-\left(\frac{\delta_o}{\delta_{tot}}\right)\right]\sigma_E \text{ and, } \delta_{tot} = (\delta_o)/[1-(\sigma/\sigma_E)] \tag{16}$$

Once yielding has fully developed, put M^{θ}_{pc} from Eq. (15) into Eq.(13) to get an expression for δ_{tot} as

$$\sigma = \left(\frac{M^{\theta}{}_{pc}}{A_o\delta_{tot}}\right) \text{ or } \delta_{tot} = \left\{\left[\frac{2(\sigma_t+\sigma_c)(R^3-r^3)}{3\pi(R^2-r^2)\sigma}\right]\right\} sin\left[\frac{\pi(\sigma_c-\sigma)}{(\sigma_t+\sigma_c)}\right] \tag{17}$$

Finally, by equating the right hand sides of Eq.(16) and Eq.(17), we arrive at the following transcendental equation for the determination of the collapse stress σ, which will be designated as $\bar{\sigma}$

$$\left\{\left[\frac{2(\sigma_t+\sigma_c)(R^3-r^3)}{3\pi(R^2-r^2)}\right]\right\}\left(1-\frac{\bar{\sigma}}{\sigma_E}\right) sin\left[\frac{\pi(\sigma_c-\bar{\sigma})}{(\sigma_c+\sigma_t)}\right] - \bar{\sigma}\delta_o = 0 \tag{18}$$

Developing Eq.(18) into a Taylor series and keeping only two terms of this series, one obtains:

$$\bar{\sigma}^2 + C\bar{\sigma} + D = 0 \text{ where } C = -\sigma_E - \sigma_c - 1{,}5\delta_o\sigma_E\left[\frac{(R^2-r^2)}{(R^3-r^3)}\right] \text{ and } D = \sigma_E\sigma_c \tag{19}$$

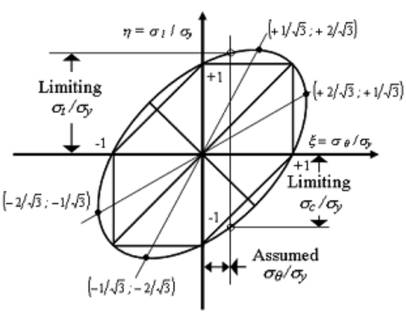

Figure 4: Von-Mises-Hencky Yelding Criterion

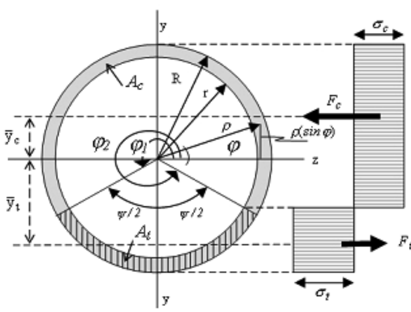

Figure 5: Idealized fully plastic stress distribution

The solution for the collapse stress $\bar{\sigma}$ in Eq.(19) takes into consideration: (a) the geometric properties of the pipe section; (b) the initial imperfection for the particular FSP; (c) an upper bound limit represented by the Euler's buckling load; (d) the fully-plastic stress distribution, (Fig.-5); (e) the fully-plastic capacity depends on both the plasticity criterion and the hoop stress, which is a function of the applied internal pressure; (f) long structures, with initial imperfection, never reach the Euler's Load (which is an upper bound limit); (g) the Euler's load (or stress) which is a function of the modulus of elasticity, pipe cross-section properties, and pipe length; and (h) the consideration of initial imperfection that is essential as it triggers the limiting fully-plastic moment capacity mechanism.

5. COMPARISON TO FINITE ELEMENT ANALYSES

For obtaining collapse load for FSPs as a function of L_i/D ratios; consider a typical pipeline for petroleum transportation with a range of free spans L_i. The material and cross section properties of the pipeline are: (a) E= 200000MPa, (b) σ_y =448MPa, (c) σ_u =531MPa, (d) D = 323.85 mm, (e) t = 19.05 mm, (f) d = 285.75 mm, (g) R = D/2 (161.925 mm), and r =d/2 (142.875 mm), and na internal pressure p = 10.2Mpa. The range of free span ratios (or L_i/D) are shown in Table 1. For each FSP length L_i, an initial imperfection δ_{oi} is assumed. In this paper, δ_{oi} is taken as the transversal deformation of the FSP such that the extreme fibers of the pipe cross section are just reaching the onset of yielding. Any other value of δ_{oi} could be arbitrarily used. For simplification, and just to calculate an initial imperfection, it was assumed that on the onset of yielding σ_t=σ_c=σ_y. Each L_i determines different Euler's load P_E and stress σ_E. The collapse loads of such FSPs without internal pressure are readily obtained and reported in Table-1. The analytical solutions are compared to Finite Element Analyses using ABAQUS [1]. It is also noticed that the analytical results reported in Table-1 consider the ultimate stress σ_u in the place of yielding stress σ_y into Eq.(6) - in the ABAQUS runs and results the ultimate stress is reached.

Table-1: Comparison with FEM results

Li/D	Initial δ_{0i}(mm)	Euler's Load & Stress		FSP Collapse(kN) With Internal Pressure		
		Euler's Load PE(kN)	Euler's Stress σ_E(Mpa)	Ultimate Stress	ABAQUS FE with Pressure	Error(%) w.r.t. ABAQUS
0	0.00	∞	∞	7871.194	NA	NA
4	2.902	2.50E+05	1.37E+04	6694.619	8041.080	-16.74
6	6.529	1.11E+05	6.09E+03	6546.097	7324.820	-10.63
8	11.607	6.25E+04	3.43E+03	6348.670	6828.900	-7.03
12	26.119	2.78E+04	1.52E+03	5844.567	5913.680	-1.17
15	40.815	1.78E+04	9.75E+02	5408.596	NA	NA
20	72.577	1.00E+04	5.48E+02	4660.695	4027.00	15.74

6. CONCLUSIONS

This paper presented a mathematical formulation regarding the investigation of compressive collapse loads of pressurized FSPs. A strategy for obtaining collapse loads as a function of the span length, initial imperfection, and fully plastic stress capacity has been presented and discussed. Examples of collapse loads, for pressurized FSPs with a variety of lengths and initial imperfections, were compared to the sophisticated FE results from the ABAQUS program. The numerical tests show that the proposed analytical formulation represents a good approximation to freespan solutions. Instead of yield stress, the analytical solutions were almost coincident with the collapse results generated by ABAQUS FE analyses. Each complex nonlinear FE run in ABAQUS took approximately 5 hours of CPU on a SUN workstation. Finally, it is noted that the scope of the present formulation is not to propose a method to substitute precise FEM modeling and analyses, but to provide an easy, faster and practical way for a first assessment of compressive collapse loads of pressurized FSPs for the petroleum industry.

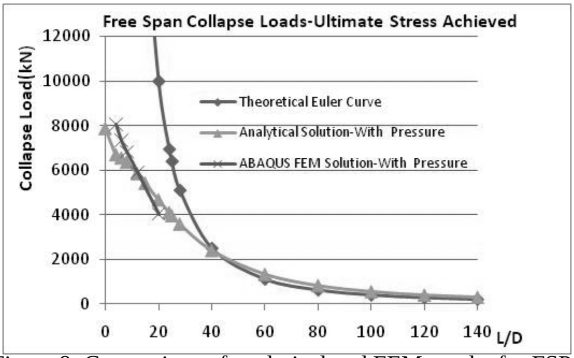

Figure 9: Comparison of analytical and FEM results for FSP

REFERENCES

[1] ABAQUS. (2000). Standard User's Manual. Version 6.3. Hibbitt, Karlsson and Sorense, USA.

[2] DOREY, A.B.. (2001). Critical Buckling Strains for Energy Pipelines. PhD Thesis, University of Alberta, Edmonton, AB, Canada.

[3] MOHAREB, M., D. W. MURRAY. (1999). Mobilization of Fully Plastic Moment Capacity for Pressurized Pipes. Journal of Offshore Mechanics and Arctic Eng., ASME. vol. 121. p. 237-241.

[4] POPOV, E. (1998), Eng. Mechanics of Solids. Prentice Hall. Englewood Cliffs, New Jersey, USA.

[5] HOFFMAN AND SACHS, (1953), Theory of Plasticity, McGraw-Hill Book Inc. New York, USA.

[6] SHANLEY, F. R. (1957). Strength of Materials. McGraw-Hill Book Company Inc. New York, USA.